STRATIGRAPHY OF ICE AND EJECTA DEPOSITS AT THE LUNAR POLES. K. M. Cannon[1], A. N. Deutsch[2], and J. W. Head III[2], [1]Department of Physics, University of Central Florida, 4111 Libra Drive, Orlando, FL 32816. Email: cannon@ucf.edu. [2]Department of Earth, Environmental and Planetary Sciences, Brown University, 324 Brook Street, Providence, RI 02906.

Introduction: Many lunar cold traps appear to host a small amount of water-ice frost on the surface [1-3]. Some authors have argued for thicker deposits buried at depth under dry regolith [4,5], but lack direct observations and questions remain [6]. Understanding ice volumes and how ice is distributed at depth is significant for reconstructing the history of volatile delivery to the poles, and for modeling potential water resources for future human explorers.

An often overlooked factor in studies of lunar ice is the huge amount of ejecta emplaced by the large craters near the lunar poles. Fig. 1 plots the expected ejecta thickness for several relevant crater sizes using scaling relations from McGetchin et al. [7]; for example, a Haworth-sized crater is expected to have emplaced >1 m of ejecta out to >150 km from its rim. The ejecta blankets of polar craters would have punctuated continuous deposition of volatiles in surrounding cold traps, creating a complex stratigraphy on a variety of spatial scales. Here, we use crater counting and computer modeling to investigate the large-scale ice-ejecta stratigraphies expected to have formed at the lunar poles.

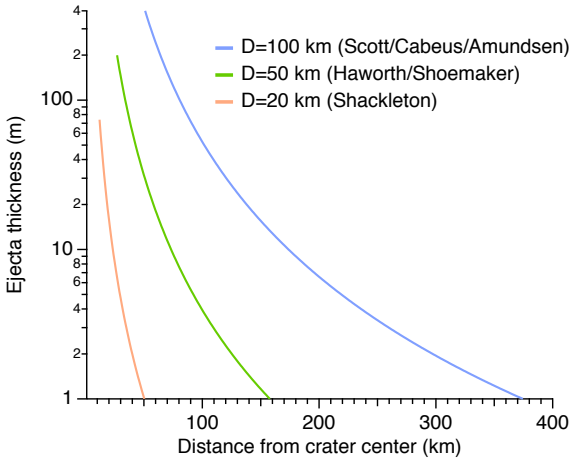

Fig. 1. Ejecta thickness as a function of distance [7] for some representative polar crater sizes.

Methods:

Crater counting. In this work we are extending the crater counting of Deutsch et al. [8] for the south pole to also include the north pole. Forty-three additional large craters were selected that have >100 km^2 of low slope (<10°) area on their floors, and are located above 80° north latitude. Crater counting is performed on a LOLA hillshade basemap [9] with 20 m horizontal resolution, with a minimum counted crater size of 200 m. The model ages are then fed into the stratigraphy modeling described below in order to place craters in time.

Ice sources. In order to model both ejecta and ice deposition, we need an idea of the amount of H_2O delivered to the lunar poles over time. In this work we consider two major sources: impact delivery from carbonaceous asteroids and from comets [e.g., 10], and volcanic outgassing [11]. For impacts, we used the present-day delivery and retention estimates from Ong et al. [10] and scaled these going back in time based on the modeled historic impact rate from [12]. For volcanism, we used the estimates from Needham and Kring [11], keeping in mind that the outgassed collisional atmosphere hypothesis faces challenges [13]. We also added additional outgassing from cryptomare using the volumes from [14]. It is not clear whether space weathering processes are net depositional [15] or net erosive [16], nor do we have data for how solar wind intensity has changed over solar system history; therefore, we leave this potential ice contribution for future work.

Stratigraphy modeling. To study the competing effects of ice deposition and crater ejecta, we created a computer model to build up representative stratigraphies. The model is a 2D grid in polar stereographic projection with a cell size of 800 m. It runs from 4.2 Ga to present with a timestep of 10 Myr. At each timestep, a layer of ice is deposited corresponding to the time-dependent delivery rates from impacts and volcanism. The ejecta from any craters of that age are also emplaced over the grid in the correct locations. We assume the total cold trap area for each pole [17] has stayed more or less constant since 4.2 Ga, with each new crater destroying some existing cold trap area but creating new cold traps as well. This allows us to calculate ice thickness based on the delivered mass, and avoids issues of accounting for paleo cold traps which no longer exist. The resulting stratigraphy of ice and ejecta is modeled at each location of the grid. It makes sense to look at the results for craters that host present-day cold traps, and to clip the columns based on our model ages.

Results: Fig. 2 shows resulting stratigraphic columns traced between three south polar cold traps: Haworth, Shackleton, and Amundsen. The results suggest that ejecta dominates the stratigraphy, with thinner interspersed ice layers, some buried at significant depths. The strata differ significantly from cold trap to cold trap

due to varying proximity to large craters, which controls the amount of ejecta present between subsequent ice horizons. However, the strata closest to the surface are more similar between different locations. We also find significant variations in the stratigraphy within individual cold traps: Fig. 3 traces the stratigraphy over three locations on the floor of Shoemaker crater, where we find up to ~100 m differences in ejecta layer thicknesses across a single cold trap.

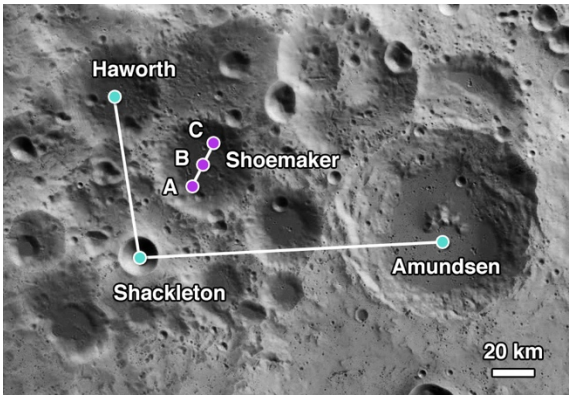

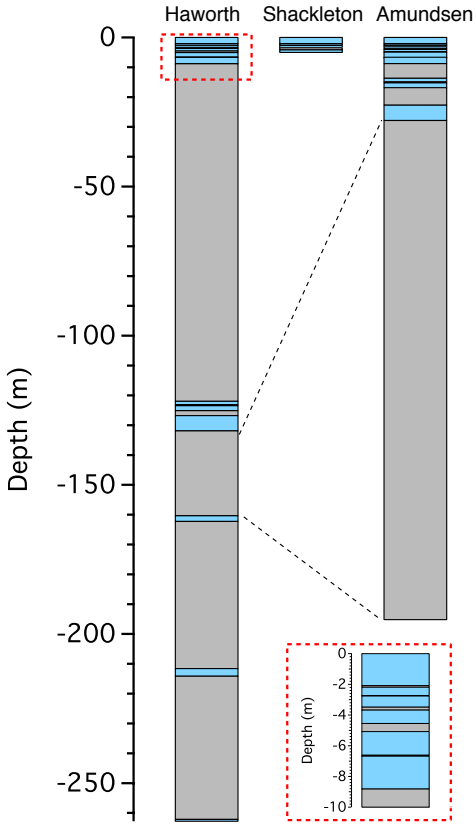

Fig. 2. Stratigraphy of ice (blue) and ejecta (gray) at three south pole craters as shown in the map above. Inset shows zoom-in of the top of the column at Haworth.

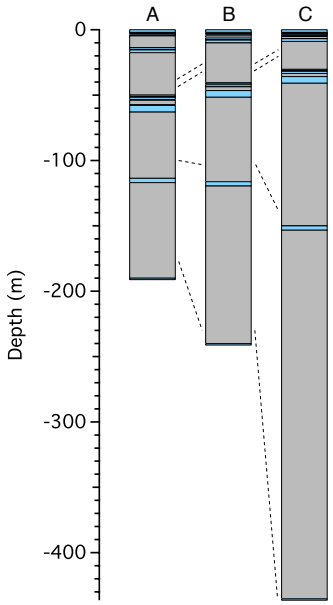

Fig. 3. Stratigraphic variation within Shoemaker crater (see map in Fig. 2).

Conclusions and Future Work: Ice at the lunar poles was not deposited on a static landscape, but a dynamic environment with hundreds of meters of ejecta emplaced around large craters formed contemporaneously with volatile delivery. The preliminary work here suggests that ejecta dominates the older strata, while ice horizons are more concentrated near the surface. We also found significant variation within individual cold traps. Future work will extend this modeling to the north pole allowing comparison with the south. We will use impact rates to estimate the extent of gardening and disruption each ice horizon likely experienced, and will consider the fate of ice during large impact events.

References: [1] Hayne P. O. et al. (2015) *Icarus*, *255*, 58. [2] Fisher E. A. et al. (2017) *Icarus*, *292*, 74. [3] Li S. et al. (2018) *PNAS*, *115*, 8907. [4] Spudis P. D. et al. (2013) *JGR*, *118*, 2016. [5] Rubanenko L. et al. (2019) *Nat. Geo.*, *12*, 597. [6] Fa W. and Eke V. R. (2018) *JGR*, *123*, 2119. [7] McGetchin T. R. et al. (1973) *EPSL*, *20*, 226. [8] Deutsch A. N. et al. (2020) *Icarus*, *336*, 113455. [9] Smith D. E. et al. (2010) *GRL*, *37*, L18204. [10] Ong L. et al. (2010) *Icarus*, *207*, 578. [11] Needham D. H. and Kring D. A. (2017) *EPSL*, *478*, 175. [12] Neukum et al. (2001) *Chron. Evol. Mars*, pp 58-86. [13] Wilson L. et al. (2019) *LPSC L*, Abstract #1343. [14] Whitten J. L. and Head J. W. (2015) *Icarus*, *247*, 150. [15] Crider D. H. and Vondrak R. R. (2002) *Adv. Space Res.*, *30*, 1869. [16] Farrell W. M. et al. (2019) *GRL*, *46*, 8680. [17] Mazarico E. et al. (2011) *Icarus*, *211*, 1066.